Enhanced Mechanistic Understanding Through the Detection of Radical Intermediates in Organic Reactions

Ivan Ocaña[a], Peter J. H. Williams[a], James Donald[a], Neil Griffin[b], George Hodges[b], Andrew R. Rickard[a,c], and Victor Chechik*[a]

Abstract: Two applications of a radical trap based on a homolytic substitution reaction (S_H2') are presented for the trapping of short-lived radical intermediates in organic reactions. The first example is a photochemical cyanomethylation catalyzed by a Ru complex. Two intermediate radicals in the radical chain propagation have been trapped and detected using mass spectrometry (MS), along with the starting materials, products and catalyst degradation fragments. Although qualitative, these results helped to elucidate the reaction mechanism. In the second example, the trapping method was applied to study the radical initiation catalyzed by a triethylboron-oxygen mixture. In this case, the concentration of trapped radicals was sufficiently high to enable their detection by nuclear magnetic resonance (NMR). Quantitative measurements made it possible to characterize the radical flux in the system under different reaction conditions (including variations of solvent, temperature and concentration) where modelling was complicated by chain reactions and heterogeneous mass transfer.

Keywords: Mass spectrometry · Mechanistic studies · Radical reactions · Radical trapping

1. Introduction

Radical chemistry holds a special place in a synthetic chemist's toolkit, thanks to the reactivity pattern which is often orthogonal to ionic reactions, and due to its good tolerance to a wide range of functional groups. Most radical reactions are chain processes requiring the addition of a small amount of thermal or photochemical (typically azo compounds or peroxides) or redox (such as Fenton reaction-based or triethylborane + air) initiator. In recent years, the development of photoredox catalysis has greatly expanded the scope of synthetic radical reactions, creating somewhat of a renaissance in their use on the laboratory scale. On paper, many of these reactions would be of interest for large scale (multi-ton) manufacturing, but their scale up is poorly understood. In general there is a lack of mechanistic understanding[1] and a complete absence of methods to measure the effects of scale on radical fluxes and radical propagation chain lengths. The main problem is that the radical intermediates generated during these organic reactions are usually too short-lived and present in too low concentrations to be observed directly by conventional analytical techniques, hence indirect methods are used. For instance, a commercially available stable nitroxide radical TEMPO ((2,2,6,6-tetramethylpiperidin-1-yl)oxyl) is often added to the reaction mixtures (Scheme 1a).[2] This stable radical rapidly reacts with carbon-centered radical intermediates, and hence inhibits radical chain reactions. In addition, the trapped radical-TEMPO adducts can often be detected by conventional analytical techniques. However, this method also suffers from disadvantages: TEMPO has limited stability; it could be involved in other radical and non-radical reactions (including initiating radical reactions), and it often combines appreciably with carbon-centered radicals.

A more general method of radical detection used in a range of different reaction systems is spin trapping (Scheme 1b).[3] This technique relies on the rapid addition of short-lived radical in-
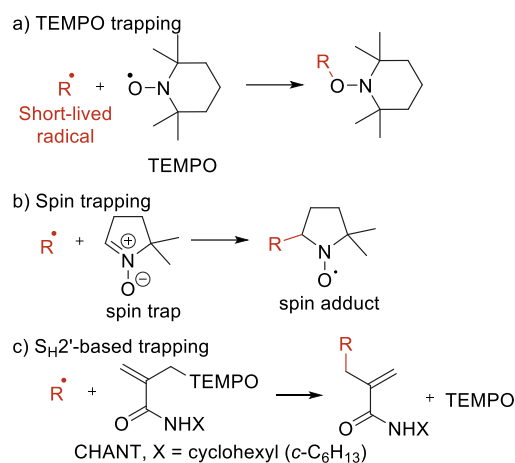
Scheme 1. Radical-trapping methodologies.

termediates to nitrone or nitroso compounds (*i.e.* spin traps) to generate persistent nitroxide radicals (*i.e.* spin adducts). The latter are typically detected by electron paramagnetic resonance (EPR) spectroscopy. However, this method often suffers from false positives; the sensitivity of EPR is sometimes insufficient for the detection of spin adducts and EPR spectra provide only limited structural information for the trapped radical.

We have recently reported a new method for the detection of free radical intermediates based on a homolytic substitution reaction (S_H2') with allyl-TEMPO derivatives (*e.g.* CHANT (*N*-cyclohexyl-2-{[2,2,6,6-tetramethylpiperidin-1-yl)oxy]methyl} acrylamide), Scheme 1c).[4] This reaction relies on a rapid addition of short-lived radicals to a terminal double bond. The product of the trapping reaction is a stable non-radical molecule which

Correspondence: Dr. V. Chechik, E-mail: victor.chechik@york.ac.uk
[a]Department of Chemistry, University of York, Heslington, York YO10 5DD, UK. [b]Jealott's Hill International Research Centre, Syngenta, Bracknell, Berkshire RG42 6EY, UK. [c]National Centre for Atmospheric Science, Wolfson Atmospheric Chemistry Laboratories, University of York, Heslington, York, YO10 5DD, UK.

can be accumulated to high concentrations and analyzed by mass spectrometry (MS) or any other conventional analytical technique. This new method resolves many of the issues associated with other trapping techniques, and has so far not led to any false positives.

Here, we give two examples of how this new method has been used to enhance mechanistic understanding of synthetically useful complex radical reactions and obtain some quantitative information about the evolution of relative radical concentrations.

2. Results and Discussion

2.1 *Radical Cyanomethylation*

Donald *et al.* have recently developed a general photochemical radical cyanomethylation reaction, using 3-azido-2-methylbut-3-en-2-ol and a Ru-based photocatalyst (Scheme 2).[5] The reaction was proposed to involve the addition of carbon-centered radical R1 to vinyl azide S3 with a radical fragmentation as a key propagation step. However, no mechanistic studies have been reported. It is an example of a complex photochemical process, and hence a good model system to demonstrate the feasibility of the new S_H2'-based method to trap short-lived radical intermediates in a complex reaction system.
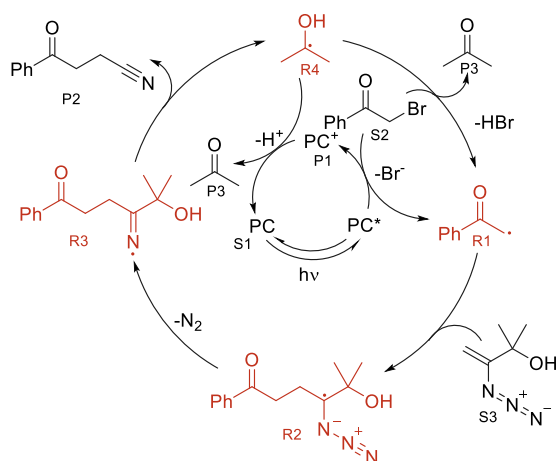
Scheme 2. Radical cyanomethylation mechanism. PC = Ru(bpy)$_3$Cl$_2$, S = substrates, R = radical intermediates, P = reaction products.

This high yielding (97%) reaction was carried out with 2-bromoacetophenone (40 mg), 3-azido-2-methylbut-3-en-2-ol (1.5 eq), 2,6-lutidine (1.5 eq) and Ru(bpy)$_3$Cl$_2$ (0.01 eq) in acetonitrile (1 mL) without and in the presence of 0.1 equivalent of the radical trap (CHANT). The reaction mixtures were analyzed by electrospray ionization mass spectrometry (ESI-MS). One advantage of MS detection is that peaks of the starting materials and products can be observed at the same time as trapped radicals and other intermediates. However, no peaks corresponding to α-bromoketone S2, vinyl azide S3 or ketone P3 (Scheme 2) were observed in this case, with starting materials not detected even before the start of the reaction. This is almost certainly due to the poor ionization efficiencies of these compounds (*e.g.* as compared to the CHANT trap) and is one of the limitations of the technique. However, peaks corresponding to the photocatalyst S1 and the desired product P2 were detected (Table 1). The product P2 peak was the strongest at the end of the reaction in absence of a radical trap but was also formed in its presence which suggested that the chain reaction was only partially inhibited. The photocatalyst S1 gave the strongest response before irradiation but significantly decreased during the reaction suggesting a degradation of the catalyst. This was confirmed by the observation of [Ru(bpy)$_2$Cl$_x$/Br$_x$]$^+$ peaks at the end of the reaction which are easily identified owing to the distinctive isotope pattern of Ru.

Peaks corresponding to radicals R1 and R4 were observed with much greater (over 30-fold) intensity at the end of the reaction as compared to the background signals at the start of the reaction (Table 1). The much higher intensity of these peaks compared to neighboring peaks (Fig. 1), coupled with the high resolution of the mass spectrometer, made their assignment unambiguous. Tandem MS further confirmed the structure of the radicals. In particular, loss of H$_2$O from the trapped R4 upon fragmentation confirmed the presence of an alcohol group in the radical structure. The peak for trapped R1 was significantly more intense than the one for trapped R4. This is likely due to a rapid consumption of R4 which can be explained by the large negative reduction potentials of α-hydroxyalkyl radicals.[6] In addition, R1 is formed earlier in the cycle and hence its trapping prevents formation of R4 thus further reducing the amount of trapped R4.

Peaks corresponding to trapped R2 and R3 were not observed. It was hypothesized that intramolecular fragmentations of R2 and R3 occurred too quickly for trapping to occur. This indicated a limitation of the new trapping method. We note, however, that this argument is equally applicable to any trapping technique.

To summarize, S_H2' trapping enabled simultaneous observations of the starting materials, products and most stable intermediate radicals in a complex process which was proposed to involve two interlocked radical chains. The results confirmed the hypothesized reaction mechanism. Simultaneous detection of the two radical intermediates and their structural assignments would have been challenging to achieve using other methods.

Table 1. MS peak intensities relative to unreacted CHANT (%).[a]

Species	After reaction without CHANT	Before reaction	After reaction
[CHANT+H]$^+$	0	100	47.2
[S1]$^{2+}$	0.348	4.05	0
[trapped R1+Na]$^+$	0	0.065	4.40
[trapped R4+Na]$^+$	0	0.025	0.773
[P1]$^{3+}$	0	0.043	0
[P2+Na]$^+$	0.024	0.002	0.011
[Ru(bpy)$_2$ClBr]$^{+\,b}$	0.024	0	0.344
[Ru(bpy)$_2$Br$_2$]$^{+\,c}$	0.350	0	19.9
[Ru(bpy)$_2$Br]$^{+\,b}$	11.3	4.42	3.25

[a] for all mixtures, this is relative to the intensity of the [CHANT+H]$^+$ peak in the "Before reaction" sample ; [b] ^{101}Ru, ^{79}Br, ^{35}Cl; [c] ^{79}Br^{81}Br.

Fig. 1. ESI-MS of trapped R1 (blue) and R4 (red).

Although qualitative results presented in this example helped to confirm the reaction mechanism, the most useful mechanistic information is quantitative. Absolute quantification of intermediate radical concentrations using any trapping methodology is challenging as the trapping reactions compete with the other reactions in the system, and the rate constants are usually not known. However, even relative radical quantification can still be very useful for comparing trends and the evolution of relative radical concentrations in related systems. In the following section, we illustrate the potential of the S_H2' radical trapping method for quantitative measurements.

2.2 Triethylborane as a Radical Initiator in Air

Autoxidation of triethylborane (Et_3B) in air became a powerful method for the initiation of radical reactions in the late 1980s.[7] Unlike conventional thermal initiators such as azo compounds or peroxides, triethylborane can be used at low temperatures in the presence of air, and the convenience of running radical reactions in aerobic conditions is also attractive.[8,9] The mechanism of triethylborane autoxidation is well understood (Scheme 3).[9,10] The initial slow (k_1) reaction with oxygen generates two radicals $Et_2BOO^\bullet$ and $Et^\bullet$. The ethyl radical is involved in the propagation step of autoxidation (Scheme 3). It reacts with oxygen extremely rapidly (k_2) generating a peroxyl radical $EtOO^\bullet$. Peroxyl radicals such as $EtOO^\bullet$ and $Et_2BOO^\bullet$ are usually relatively stable, however they react with boranes several orders of magnitude faster than with other carbon-based molecules. This is the main factor that makes triethylborane such an efficient radical initiator. Thus, a fast (k_3) reaction of $EtOO^\bullet$ with Et_3B generates another ethyl radical which completes the propagation chain. As the autoxidation cycle rapidly consumes oxygen, the reaction mixture becomes deoxygenated and the $Et^\bullet$ radical acts as an initiator of the target radical process.
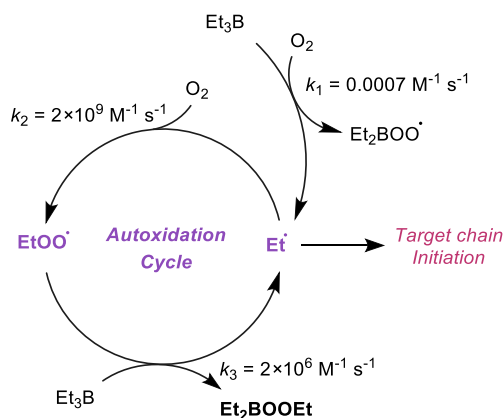
Scheme 3. Mechanism of autoxidation of triethylborane.

Although approximate rates of reactions for the Et_3B autoxidation are known, the reaction critically depends on oxygen concentrations (usually determined by oxygen solubility in the reaction mixture) and oxygen diffusion which are very difficult to model. Therefore, optimization of these reactions often relies on empirical kinetic data. We applied S_H2' trapping to obtain quantitative mechanistic information about the Et_3B autoxidation cycle.

The reactions in Scheme 3 are so selective that we observed clear signals of trapped ethyl radicals in ^1H NMR spectra of crude reaction mixtures (Fig. 2). This made it possible to quantitatively monitor reaction progress. We note that each radical trapping event releases a molecule of TEMPO which also reacts with $Et^\bullet$ very rapidly (Scheme 1a), hence the NMR spectra show both trapped ethyl radicals and Et-TEMPO adduct.
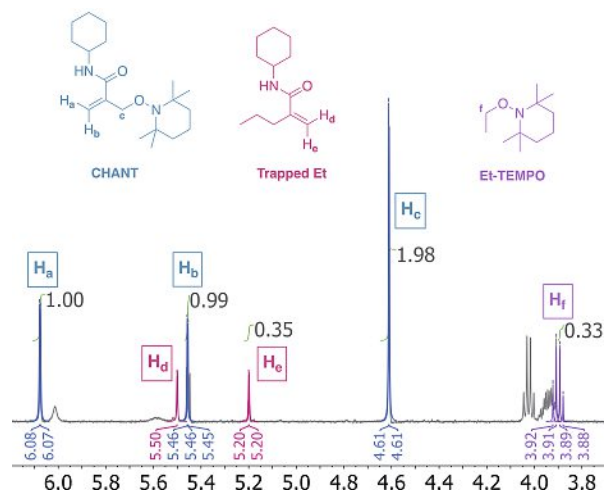
Fig. 2. ^1H NMR spectrum of Et_3B autoxidation in the presence of CHANT radical trap in the 3.7-6.2 ppm range.

Initial experiments were aimed at the optimization of the radical flux by changing the concentrations of the starting materials. Reagents in 1 mL of *n*-hexane were added to an NMR tube in an inert atmosphere, the mixture was evacuated, and air was introduced in the headspace of the tube (this amount was sufficient to completely oxidize Et_3B at $[Et_3B]$ = 25 mM). The solution was left unstirred. This protocol made it possible to reduce variability in the rate of oxygen dissolution, eliminate uncontrolled mixing, and obtain reproducible results, which could be used for quantitative comparison of reactions run under different conditions. The results were analyzed by ^1H NMR after 16 h (Table 2). This simple experiment showed significant variation in the amount of trapped ethyl radicals and demonstrated the potential of S_H2' trapping to obtain quantitative reactivity trends. The apparent lack of correlation between trapped Et radicals and Et_3B concentration highlights the complexity of this radical chain process, which strongly depends on the rate of oxygen diffusion from the gas phase into the reaction medium.

Table 2. Concentrations of CHANT-trapped Et radicals under different reaction conditions[a].

CHANT / mM	Et_3B / mM	Trapped Et[b] / mM
25	25	13.6
25	100	9.4
6.2	25	6.6
6.2	100	6.4

[a]The concentrations of trapped Et radicals were determined by ^1H NMR after complete conversion of Et_3B. [b]Trapped ethyl radicals and Et-TEMPO adduct combined.

The evolution of reaction components was then monitored by NMR over time (Fig. 3). By recording both ^{11}B and ^1H spectra, we were able to simultaneously track the concentrations of several reaction components, including trapped radicals.

Triethylborane initiations are sometimes run at temperatures as low as –78 °C. The effect of temperature on the reaction would be very difficult to model, not least because increased solvent viscosity at low temperatures will significantly slow down both diffusion-controlled radical reactions and the diffusion of oxygen through the reaction medium. In order to probe the efficiency of initiation at low temperatures, the experiment was repeated at
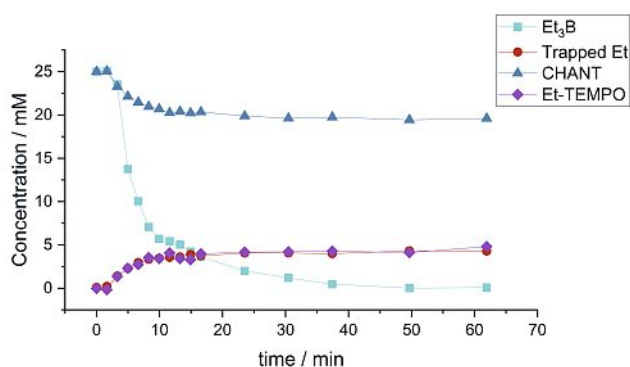
Fig. 3. Kinetic profile for the oxidation of Et$_3$B (25 mM) by air at 25 °C in the presence of CHANT (25 mM) in 1 mL of *n*-hexane. The reaction was followed by ¹H and ¹¹B NMR spectroscopy and measurements were taken at the indicated timestamps.
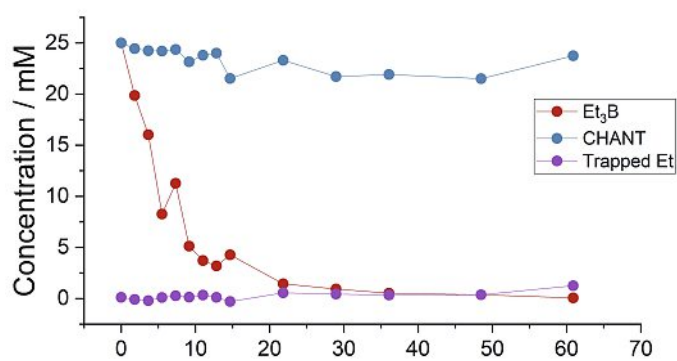
Fig. 4. Kinetic profiles for the oxidation of Et$_3$B (25 mM) at –50 °C in the presence of CHANT (25 mM) in 1 mL of *n*-hexane. The reaction was followed by ¹H and ¹¹B NMR and measurements were taken at the indicated timestamps. Et-TEMPO peaks (H$_f$, Fig. 2) were not sufficiently resolved to monitor at –50 °C.

Table 3. Solvent effect on Et radical trapping in the oxidation of Et$_3$B (25 mM) by air at 25 °C in the presence of CHANT (25 mM) in 1 mL of different solvents, as monitored by ¹H and ¹¹B NMR spectroscopy.

Solvent	Reaction time, h[a]	Trapped Et[b] / mM
Hexane	0.12	13.6
THF	0.38	2.5
Toluene	0.83	6.5
DMF	8	5
DCE	80	2.5

[a]Time corresponding to 50% consumption of Et$_3$B; [b]Trapped ethyl radicals and Et-TEMPO adduct combined, measured after complete Et$_3$B consumption.

–50 °C. This temperature was chosen as it still gives relatively sharp NMR peaks required for quantitative measurements.

The reaction profile for the oxidation of Et$_3$B with air at –50 °C (Fig. 4) aligns with that at room temperature, as the triethylborane reacts with similar rates at both temperatures. This can be attributed to two factors acting in opposite directions. The lower temperature slows down the rate of oxygen diffusion and the rates of reactions described in Scheme 3. However, the solubility of O$_2$ increases at lower temperatures, thereby accelerating the oxidation rate. The interplay of these two processes results in a similar reaction profile at the two temperatures.

Upon completion of the reaction, the concentration of trapped ethyl radicals (a sum of CHANT-trapped ethyl radicals and Et-TEMPO adduct) was *ca.* 2.5 mM, a significant reduction compared to the 13.6 mM observed at room temperature. This shows a significant decrease in initiation efficiency at lower temperature under the given reaction conditions (*i.e.* no stirring). It is possible that the trapping of ethyl radicals is outcompeted at lower temperatures by the reaction with oxygen present at high concentration. This results in less initiation at the same level of oxidation.

Et$_3$B is a strong Lewis acid and its interactions with even weak Lewis base solvents are likely to strongly affect kinetics of its reactions. There is however no literature data on the solvent effect on Et$_3$B radical initiation. To obtain some empirical data, we studied S$_H$2' trapping for the Et$_3$B autoxidation in different solvents (Table 3).

As anticipated, the choice of solvent had a significant effect on the autoxidation rate. The half-reaction time dramatically increased from *ca.* 7 min in hexane to 80 h in dichloroethane. This substantial variability can be tentatively attributed to the stabiliz-

ing interaction between Et$_3$B and solvents with some Lewis basicity. Such interaction would decrease the reaction rate which is consistent with the reactivity trend observed for hexane, THF, toluene and DMF. However, the very slow oxidation of Et$_3$B in dichloroethane remains unexplained. Interestingly, this reaction also proceeds very slowly in 1,2-dichlorobenzene, suggesting that chlorine-containing solvents strongly inhibit the autoxidation of Et$_3$B. Reactivity trends should be treated with caution as they also depend on solubility of oxygen and solvent viscosity (which determines the rate of oxygen diffusion).

The total amount of trapped radicals (determined after complete consumption of Et$_3$B) also varied significantly in different solvents (Table 3). Hexane gave the highest concentration of trapped ethyl radicals (13.6 mM). This was followed by toluene, which had half the concentration of trapped radicals (6.5 mM), DMF was third (5 mM), and finally, THF and DCE gave the lowest concentration of trapped ethyl radicals (2.5 mM). It is difficult to unambiguously explain this solvent effect. A small perturbation of relative reaction rates in a chain reaction can result in significant changes in the overall product ratios. Certain factors however can be used to tentatively explain the observed reactivity. Solvents with labile hydrogens such as THF, can undergo hydrogen atom transfer (HAT), to form THF-based radicals that will be captured by CHANT and TEMPO. Both of these species were observed during MS analysis of the reaction mixtures. Radical capture by solvents reduces both the steady state concentration of ethyl radicals, and the amount of unreacted trap available for trapping ethyl radicals thus explaining lower trapping efficiencies in these solvents.

In many real reaction mixtures, concentrations of trapped radicals will be too low to be detected by NMR, therefore ESI-MS, perhaps in combination with liquid chromatography (LC), will have to be used. Accurate quantification of ESI-MS data is best achieved using isotopically labelled compounds. However, this is likely to be prohibitively expensive in most cases. An alternative, but time-consuming approach uses standard additions of authentic compounds to the reaction mixtures. A somewhat less accurate but faster and more accessible approach is to build calibration curves for LC-MS quantification using solutions of authentic compounds at different concentrations. Fortunately, the products of S$_H$2' trapping are stable compounds (alkenes) which are commercially available or can be relatively easy to synthesize. In order to test the feasibility of determining trapped radical concentrations using LC-MS, we reanalyzed triethylborane autoxidation mixtures by LC-MS and built calibration curves using an authentic product of CHANT- Et• trapping.

The robust correlation (r² = 0.999) and reproducibility (RSE = 0.5%) of the external calibration curve suggest that LC-MS analy-
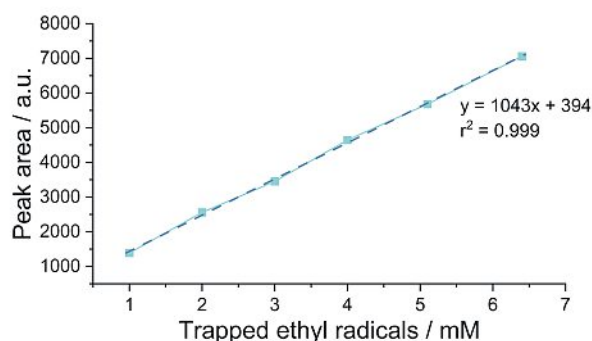
Fig. 5. LC-MS external calibration curve prepared using pure CHANT-Et·product.

sis can be employed to quantify trapped ethyl radicals within the studied concentration range (Fig. 5).

A good separation of trapped ethyl radicals from most other compounds present in the mixture was achieved in LC-MS chromatograms. In most solvent systems, NMR and LC-MS results showed acceptable agreement suggesting that the latter method could be used to at least estimate the concentrations of trapped radicals in reaction mixtures (Table 4). This method however needs to be used with caution; relatively large differences between NMR and LC-MS results in THF and hexane is likely due to incomplete LC separation of trapped ethyl radicals from other compounds and high sensitivity of the MS ionization efficiency to the chemical composition of the analyte. The use of standard addition and/or isotope labelling would be required to increase the accuracy of the LC-MS analysis.

Table 4. Quantification of trapped ethyl radicals using NMR and LC-MS. The oxidation of Et_3B (25 mM) at 25 °C in the presence of CHANT (25 mM) in 1 mL of solvent was followed by ^1H and ^{11}B NMR. Trapped ethyl radicals were measured after Et_3B consumption. The same samples were then analysed by LC-MS.

Solvent	NMR / mM Trapped Et·	LC-MS / mM Trapped Et·
Hexane (25 °C)	6.8	9.4
Hexane (–50 °C)	1.3	2.6
Toluene	3.3	3.6
THF	1.3	2.5
DMF	2.5	1.7
DCE	1.2	1.9

3. Conclusions

The examples given above demonstrate the utility of the new S_H2' radical trapping method in complex chemical systems, and how the mechanistic details and the radical flux quantification required for an understanding-based scale up can be gained. We believe these methods can also be applied to reactions run across scales including in typical process equipment (so long as sampling is possible) using standard analytical techniques readily available at most Process Development sites.

4. Experimental

Radical Cyanomethylation

CHANT and 3-azido-2-methylbut-3-en-2-ol were synthesized as described in literature[4,5] and the trapping procedure was adapted from a trap less literature procedure.[5] 2-Bromoacetophenone (40.0 mg, 200 μmol, 1.00 eq.), 3-azido-2-methylbut-3-en-2-ol

(38.1 mg, 300 μmol, 1.50 eq.), 2,6-lutidine (32 mg, 35 μL, 300 μmol, 1.50 eq.) and Ru(bpy)$_3$Cl$_2$·6H$_2$O (1.5 mg, 2.0 μmol, 0.01 eq.) were placed in a transparent 2 mL vial and dissolved in MeCN (1.0 mL). When undertaking radical trapping, CHANT (12.9 mg, 40 μmol, 0.20 eq.) was also added. An aliquot was then removed (0.10 mL) and the remaining solution sparged with argon for 10 min, whilst stirring. This reaction mixture was irradiated with blue LEDs (60 W, 455 nm) for 4 h, whilst stirring. Another aliquot was then removed (0.10 mL). All aliquots had solvent removed *in vacuo* and were redissolved in 0.1 % HCOOH/1:1 MeCN:H$_2$O and characterized using positive ESI-MS on a high resolution solariX XR FTMS (solariX) mass spectrometer (m/z ±0.0001 precision, >107 maximum resolution, mass accuracy 600 ppb (internal)). Tandem MS was undertaken as required.

Et_3B Autoxidation

CHANT (8 mg, 25 μmol, 1 eq.) was dissolved in the corresponding solvent (1 mL) and transferred into an NMR tube. The solution was degassed using freeze-pump-thaw and backfilled with N$_2$. The tube was brought inside the glovebox and Et$_3$B (1 M in hexanes, 25 μL, 25 μmol, 1 eq.) was added. The sealed tube was taken outside the glovebox and freeze-pump-thawed again, leaving the headspace at reduced pressure (≈ 20 mbar). ^{11}B and ^1H NMR spectra were recorded before opening the tube to air and sealing it again. The reaction was monitored by ^{11}B and ^1H NMR spectroscopy until complete consumption of Et$_3$B. The NMR tube was left in the instrument for the duration of the reaction, and absolute NMR integrals were used for quantification. Control experiments showed that the drift in NMR intensity was within 1% under these conditions. Solvent (hexane) NMR peaks were well separated from the other peaks in the spectra and solvent suppression was not necessary for quantitative analysis.

LC-MS Analysis of Et_3B Autoxidation Samples

Samples (10 μL) were dissolved in degassed MeCN (1 mL). Diluted solutions (3 μL) were then injected into an Agilent 1200 HPLC equipped with a CORTECS T3 Column (120 Å, 2.7 μm), running a gradient of 30% MeCN/H$_2$O to 60% MeCN/H$_2$O over 30 min and infused into the solariX spectrometer.

2-Methylenepentenoic Acid

Pyrrolidine (170 μL, 0.2 eq., 2.05 mmol), formaldehyde (37% in H$_2$O, 0.8 mL, 2 eq., 20.52 mmol) and 2-propylmalonic acid (1.55 g, 1 eq., 10.26 mmol) were dissolved in ethanol (35 mL). The mixture was heated to reflux for 18 h. The volatiles were removed *in vacuo* and the solution was diluted in H$_2$O (30 mL) and acidified with aq. HCl to pH 3-4. The solution was extracted with EtOAc (3×30 mL) and the combined organic phases were washed with brine (40 mL), dried over MgSO$_4$ and filtered. The solvent was removed *in vacuo* to give the desired product 2-methylenepentenoic acid (1.11 g, 95% yield) as a yellow oil.

^1H NMR (400 MHz, CD$_3$OD) δ 6.13 (d, J = 1.8 Hz, 1H), 5.56 (d, J 1.8 Hz, 1H), 2.26 (t, J 7.3 Hz, 2H), 1.59 – 1.43 (m, 2H), 0.93 (t, J 7.4 Hz, 3H).

^{13}C NMR (101 MHz, CD$_3$OD) δ 170.61, 142.47, 125.37, 35.01, 22.81, 13.97.

MS (+ve ESI): *m/z* 114.068 ([M+H]$^+$, 100%).

N-Cyclohexyl-2-methylenepentanamide (Trapped Ethyl Radical)

2-Methylenepentoic acid (1.11 g, 9.67 mmol, 1.0 eq.) was dissolved in N,N-dimethylformamide (DMF, 50 mL). Cyclohexylamine (1.05 g, 10.28 mmol, 1.0 eq.), N,N,N′,N′-tetramethyl-O-(1H-benzotriazol-1-yl)uronium hexafluorophosphate (HBTU, 4.5 g, 11.87 mmol, 1.1 eq.) and N,N-diisopropylethylamine (DIPEA, 2.75 g, 21.27 mmol, 2.0 eq.) were added and the solution was stirred at room temperature for 24 h. Saturated NaHCO$_3$ solu-

tion (40 mL) was added and the formation of a precipitate was observed. This was dissolved by adding H_2O (100 mL). The mixture was extracted with EtOAc (3×70 mL) and the combined organic phases were washed with brine (3×40 mL), dried over $MgSO_4$ and filtered. The solvent was removed *in vacuo* to give an orange oil. The oil was purified by flash silica column chromatography (20% EtOAc/hexanes, R_f 0.37) to give the desired product N-cyclohexyl-2-methylenepentanamide as a white solid (1.38 g, 73% yield).

^{1}H NMR (400 MHz, $CDCl_3$) δ 5.62 (s, 1H), 5.53 (s, 1H), 5.21 (s, 1H), 3.88 – 3.74 (m, 1H), 2.27 (t, J 7.7, 1.4 Hz, 2H), 1.93 (dt, J 11.9, 4.0 Hz, 2H), 1.97 (dq, J 11.9, 3.9 Hz, 2H), 1.81 – 1.67 (m, 2H), 1.66 – 1.57 (m, 1H), 1.52 – 1.42 (m, 2H), 1.22 – 1.10 (m, 3H), 0.92 (t, J 7.3 Hz, 3H).

^{13}C NMR (101 MHz, $CDCl_3$) δ 168.30, 146.21, 116.81, 48.25, 34.60, 33.26, 25.68, 24.97, 21.38, 13.86.

MS (+ve ESI): *m/z* 196.1696 ([M+H]+, 16%), 218.1515 ([M+Na]+, 100%).

[1] S. J. Horsewill, G. Hierlmeier, Z. Farasat, J. P. Barham, D. J. Scott, *ACS Catal.* **2023**, *13*, 9392, https://doi.org/10.1021/acscatal.3c02515.
[2] T. Vogler, A. Studer, *Synthesis* **2008**, *13*, 1979, https://doi.org/10.1055/s-2008-1078445.
[3] E. G. Janzen, *Acc. Chem. Res.* **1971**, *4*, 31, https://doi.org/10.1021/ar50037a005.
[4] P. J. H. Williams, G. A. Boustead, D. E. Heard, P. W. Seakins, A. R. Rickard, V. Chechik, *J. Am. Chem. Soc.* **2022**, *144*, 15969, https://doi.org/10.1021/jacs.2c03618.
[5] J. R. Donald, S. L. Berrell, *Chem. Sci.* **2019**, *10*, 5832, https://doi.org/10.1039/C9SC01370A.
[6] T. Lund, D. D. M. Wayner, M. Jonsson, A. G. Larsen, K. Daasbjerg, *J. Am. Chem. Soc.* **2001**, *123*, 12590, https://doi.org/10.1021/ja011217b.
[7] K. Nozaki, K. Oshima, K. Uchimoto, *J. Am. Chem. Soc.* **1987**, *109*, 2547, https://doi.org/10.1021/ja00242a068.
[8] D. F. J. Caputo, C. Arroniz, A. B. Dürr, J. J. Mousseau, A. F. Stepan, S. J. Mansfield, E. A. Anderson, *Chem. Sci.* **2018**, *9*, 5295, https://doi.org/10.1039/C8SC01355A.
[9] D. P. Curran, T. R. McFadden, *J. Am. Chem. Soc.* **2016**, *138*, 7741, https://doi.org/10.1021/jacs.6b04014.
[10] A. G. Davies, *J. Chem. Res.* **2008**, *361*, https://doi.org/10.3184/030823408785702526